Characterization of low alloy steel impregnated with WS_2 using nano-indentation

Suresh R. Ambalam*, Rajendran I. Gounder

Department of Mechanical Engineering, Dr. Mahalingam College of Engineering, and Technology, (An autonomous institute affiliated to Anna University, Chennai, India) Udumalai Road, Pollachi, 642003, India

*Corresponding author, Tel: (+91) 9442765776; E-mail: arsuresh2005@gmail.com

Received: 21 March 2016, Revised: 30 September 2016 and Accepted: 20 December 2016

DOI: 10.5185/amp.2017/302
www.vbripress.com/amp

Abstract

Low alloy steel is used in industrial applications to manufacture bearing materials, bushes, gears, etc. In this work, an attempt has been made to characterize powder metallurgy (PM) processed low alloy steel impregnated with solid lubricant WS_2 in four different weight proportions (0, 2.5, 5 and 10%) using nano-indentation. Results of nano-indentation were correlated with impregnated quantity of WS_2 and micro structural phases in sintered low alloy steel. The values of elastic moduli and contact stiffness were found to be higher in the PM-processed low alloy steel impregnated with WS_2 compared with the low alloy steel without WS_2. Ferritic and pearlitic phases in the microstructure were observed in low alloy steel impregnated with 0 % WS_2. Larger proportion of martensitic phase was observed in the microstructure of low alloy steel impregnated with 5 and 10 % of WS_2. The specimen with 2.5 % WS_2 by weight has the highest hardness and the highest elastic modulus of all the proportions tested, which may be attributed to predominant bainitic structure present in it. Hence the PM-processed low alloy steel impregnated with 2.5 % WS_2 would be more suitable composition for manufacturing sliding members due to its superior mechanical properties.

Keywords: Nano-indentation, powder metallurgy, low alloy steel, solid lubricant, phase transformation.

Introduction

Sliding pair is to be made of suitable material combination for durability. To minimize wear of the components in sliding applications, techniques to retain lubricant at the contact interface are in practice. Oil pockets on the sliding face of the components are used for retaining lubricant. To improve the wear behaviour of the component, dimples on sliding face are made to facilitate retention of lubricant [**1**]. Laser Surface Texturing (LST) on the sliding face of the component is widely employed to create dimples. Reduction of friction losses was reported with LST on a flat ring than non LST ring [**2**]. Reduced fuel consumption was reported with Partial Laser Surface Texturing (PLST) on piston ring surface compared to non-PLST rings [**3**].

Manufacturing sliding components through PM (Powder Metallurgy) route offers distinct advantage of inherent porous structure which facilitates retention of lubricant. Admixing materials selectively during compounding, chance to manufacture components with controlled porosity to suit the application needs and the ability to manufacture near net-shaped products which minimize further processing needs are the unique advantages of processing through PM route [**4**]. In addition to retaining lubricant, porous structure of PM components traps wear debris and influences wear resistant characteristics [**5**]. Under dry sliding condition, porous-PM components offer better wear resistance compared with non PM-processed stainless steel [**6**]. But porous structure in PM components may also act like micro cracks and initiation points for crack growth/crack propagation, which may accelerate creation of wear debris. In sinter-hardened steels, pores initiate formation of several micro-cracks that were joined to form more than one macro crack [**7**]. Admixing solid lubricant in PM products, offers distinct advantage to reduce wear in components for sliding applications. Impregnation of solid lubricant like MoS_2 in PM products avoids adverse chemical reactions and oxidation problems associated if added in melting stage. For better wear resistance and frictional properties, uniform distribution of solid lubricant in PM-processed components is used. PM-processed specimens impregnated with oil have reduced wear [**8**]. Alloying elements like Cr, Ni and Mo in PM-processed low-alloy steels have strong influence on the tensile and impact properties [**9**].

For validation of materials before scaling up for production, pellets usually smaller in dimensional sizes are produced. To measure mechanical properties of small specimens, nano-indentation

has become very popular and significant experimental technique. Nano-indentation gives direct measurement of mechanical properties of small sized specimens and surface coatings [**10, 11**]. Unlike large indenters which require large force, nano-indentation requires very small force to study about mechanical properties and the indentation creep is correlated with the maximum depth of indentation and hardness [**12**]. Stable plastic flow is observed in crystalline metals due to the motion and mutual interaction of dislocations which give rise to work hardening mechanisms. In the nano-indentation tests, even martensite in the base metal softens [**13, 14**].

The selection of right indenter geometry plays significant role in the material characterization using nano-indentation technique. It has been reported that indenter geometry influences the load–indentation depth curve, hardness and elastic modulus significantly [**15**]. Deviations from the perfect Berkovich geometry were observed due to rounding-off of indenter tip and the deformation of the indenter during indentation [**16**]. The size of indenter has significant effect on the results of measurement. Hardness decreases with the increase of indentation depth due to nano-indentation size effect [**17**]. In nano-indentation, at local scale in a single experiment, Young's modulus (E) and Poisson's ratio (ν) of an isotropic material are measured simultaneously [**18**]. For material characterization of PM-processed parts, nano-indentation technique was used successfully [**19**]. Moreover, the same technique was successfully used to study complicated heterogeneous multi-phase materials [**20**].

The novelty of this work is that an attempt is made to characterize PM-processed low alloy steel impregnated with WS_2 using nano-indentation. The objectives of this work are to study the effect of WS_2 impregnation in the micro structure of PM-processed low alloy steel, to determine fundamental mechanical properties of PM-processed low alloy steel impregnated with WS_2 using nano-indentation and to assess the results on nano-indentation and its correlation with micro structural phase changes effected by the impregnated WS_2 in the PM-processed low alloy steel.

Experimental

Materials

In this work, commercially available low alloy steel powder manufactured by M/s Hoganas AB under the trade name of Distaloy AB as given in **Table 1** with a minimum elemental purity of 99 weight percent was admixed with different proportions of WS_2. The solid lubricant WS_2 was sourced through M/s Sajan Overseas Pvt Ltd., India and it was found to have flaky structure with a minimum purity of 98 weight percent.

The constituent metal powders were used as received from commercial sources without further purification.

Table 1. Chemical composition of low alloy steel powder.

% by weight	%C	%Ni	%Mo	%Cu	%Fe
	0.2	1.7	0.45	1.5	Rest

Preparation of metal powders

Ball milling was carried out for size reduction of the powders and also for uniform admixing of WS_2 under ambient conditions.

Ball milling was carried for 30 minutes for mixing and uniform distribution of low alloy steel powder with different weight proportions of solid lubricant WS_2 (2.5, 5 and 10%). Kenolube of 0.6 % was added for lubricating effect during cold compaction and to facilitate easy removal of the green compact from the die and also to minimise wear of the tooling. Uniform distribution of WS_2 in the compounded powder mixture was ascertained with Scanning Electron Microscopy (SEM) micrographs before compacting, and distribution of WS_2 was found to be uniform and also in increasing order corresponding with mixed quantity of WS_2. Die and punch were made from D4 die steel and with the required fits and tolerances to compact pellets of 20 mm diameter

Preparation of pellets

Milled powder was filled inside the die cavity by calculating weight required for pellets duly considering allowances required for grinding and polishing after sintering for the purpose of characterization. Compaction of powders under room temperature was done using 200T hydraulic press which was equipped with arrangement of pressure and speed control. Pressure was applied to 600 MPa to get the green compact with sufficient strength for safe handling without getting crumbled. Sintering cycle was done using mesh belt furnace in a nitrogen atmosphere consisting of preheating zone, sintering zone and cooling zone. Nitrogen environment results in the structural transformation of iron powders [**21**]. Sintering was performed with a maximum furnace temperature of 1120º C to get proper diffusion bonding of atoms and the densification of the pellet. These pellets were produced without any deformity and scaling on the surface

SEM micrography

The surface of consolidated pellets was finished with 1µ emery sheet and polished with diamond paste applied onto velvet cloth for the purpose of taking SEM micrographs. With Secondary Electron Imaging (SEI) mode of SEM, high magnification micrographs of sintered specimens at a magnification of 1000X were taken. With SEM micrographs in **Fig. 1(b), (c)** and **(d)**, it was observed that distribution of WS_2 was

uniform throughout the pellet. It was noted that higher amount of WS_2 distribution in low alloy steel specimen was seen with the increasing proportion of WS_2. The morphology of different phases remained the same in all three compositions having WS_2 and the reference specimen (**Fig. 1(a)**) with only exception of increasing amount of impregnated WS_2 in the specimens. Higher amount of porous structure was observed with the increasing proportion of WS_2.

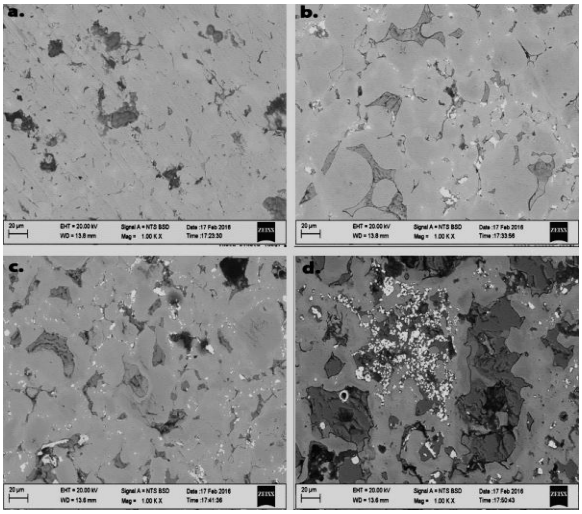

Fig. 1. SEM Micrographs of Sintered specimens.

The densities of sintered specimens were found to be 6.545, 6.884, 7.211 and 6.286 g/cm^3 for low alloy steel impregnated with '0, 2.5, 5 and 10% of WS_2 respectively. The densities of sintered specimens were found to be increasing with the increase in the amount of WS_2 up to 5 % then decreases with the further addition of WS_2 due to increase in porosity. Mechanical characterization was done with 'as sintered' specimens with varying compositions of WS_2.

Optical micrographs

Evaluation of distribution of WS_2 in the composite was done using (*Olympus Model BX51M-N33MD* Upright metallurgical optical microscope) integrated with computer-based *Metal Plus* image analysis software. All the four specimens were ground and polished with 1µ emery sheet. Diamond paste applied on to velvet cloth was used to finish-polish the specimens. Before taking micrographs, all the specimens were etched with 2% Nital (2 % by volume of HNO_3 in ethanol). Random sample micrographs at a magnification of 1000X were taken at six different locations. The average of the volume fraction of WS_2 in the specimens was found to be in close agreement with the WS_2 added before sintering.

All the phases were observed in different shades in the micrographs. It was observed from **Fig. 2** that the quantity of added solid lubricant WS_2 in low alloy steel had significant influence on the creation of new phases in the microstructure. Ferritic and pearlitic phases were observed in low alloy steel impregnated with 0 % WS_2 (**Fig. 2(a)**). Impregnating with 2.5 % WS_2 had resulted in bainitic structure predominantly in the microstructure **Fig. 2(b)**. In case of low alloy steel specimens impregnated with 5 and 10% of WS_2, martensitic phases in the microstructure were observed (**Fig. 2(c)** and **Fig. 2(d)**).

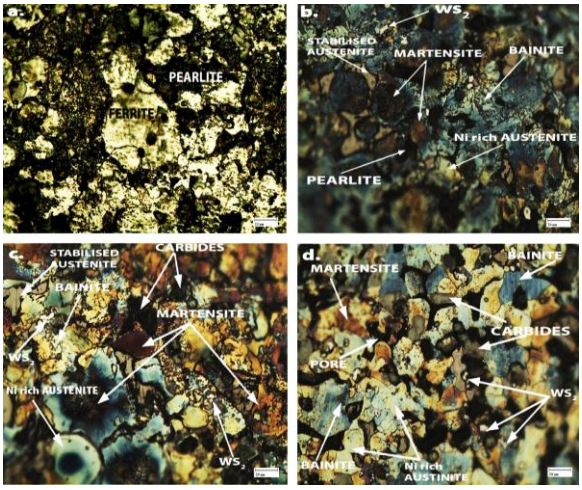

Fig. 2. Optical Micrographs of Sintered specimens.

Energy-dispersive X-ray spectroscopy (EDS)

The EDS analysis of sintered specimens was done with three iterations to confirm the presence of various elements and chemical characterization. The EDS results obtained in the sintered specimens of varying compositions are depicted in the **Fig. 3**. EDS results of low alloy steel show peaks of Fe, Cu, Ni and Mo confirming the composition of the steel. EDS results of WS_2-impregnated specimens show peaks of W and S in addition to those of Fe, Cu, Mo and Ni.

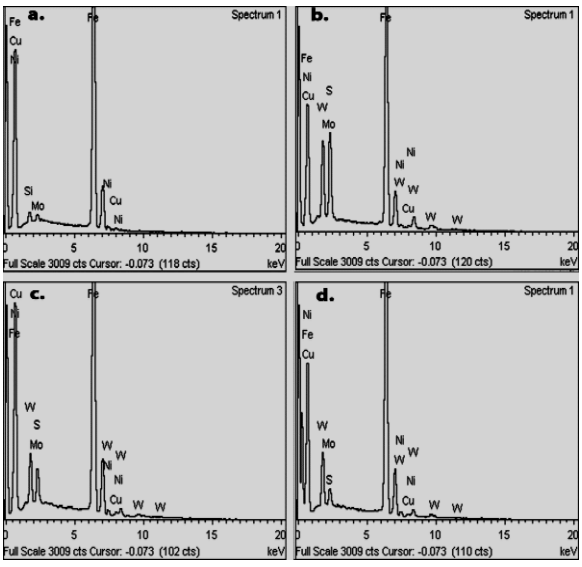

Fig. 3. EDS Spectra of sintered specimens.

X-ray diffraction (XRD)

To ensure the required diffusion bonding and chemical reaction in the sintering process, XRD

analysis was carried out after polishing the specimens to metallographic level. XRD micrographs in the angle range of 0º - 80º were taken with Shimadzu Lab-X XRD – 6000 machine with Cu source. The diffractogram analysis confirmed completion of sintering cycle with the expected chemical reaction and diffusion bonding.

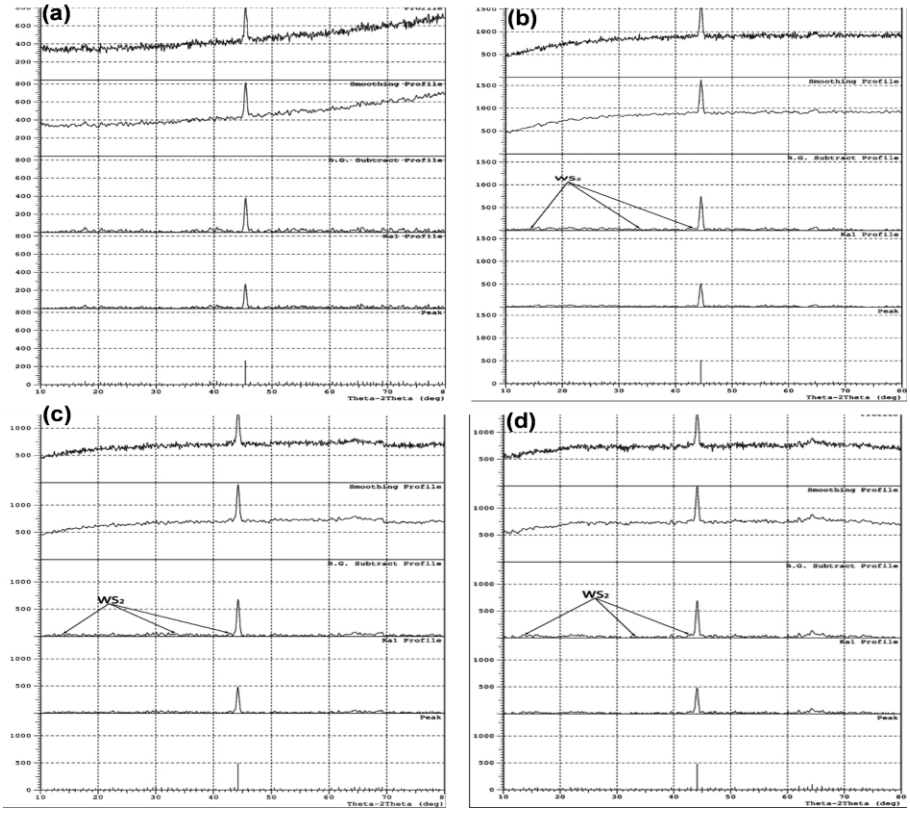

Fig. 4. (a) XRD diffractogram of on low alloy steel without WS2; (b) XRD Diffractogram of on low alloy steel with 2.5% WS2. (cont.); (c) XRD Diffractogram of on low alloy steel with 5% WS2; (d) XRD Diffractogram of on low alloy steel with 10% WS2.

The XRD pattern as given in **Fig. 4(a)** suggests the phases Ni rich ferrite matrix and pearlite phases. The predominant peaks at 44.8º in the XRD patterns of the sintered specimens confirm the presence of α-Fe in all the compositions. The peaks at 51.8º in the XRD patterns of the sintered specimens confirm the presence of Ni. Presence of copper in the specimens was confirmed from the peaks close to 50.5º in the XRD patterns. From the peaks at 14.3º, 33.5º and 43º in the X-ray diffraction pattern, the presence of hexagonal structured polycrystalline WS_2 was confirmed in the WS_2 impregnated specimens (**Fig. 4(b), (c)** and **(d)**) and it is in close agreement with JCPDS-08-0237.

Results and discussion

Nano-indentation technique

The principal goal of nano-indentation testing is to extract elastic modulus and hardness of the specimen using the Oliver and Pharr method. In nano-indentation on the surface of test material with Berkovich nano-indenter, the impression with a prescribed loading and unloading profile gives rise to shear bands as a series of steps around the periphery of the indentation. Grain orientation influences hardness and pileup patterns on the indented surfaces using Berkovich indenter [**22**]. Hardening effect in close proximity of a grain boundary was observed in nano-indentation experiments [**23**]. In this work, Nano-indentation was done using Hysitron T 1 700 UBL 1 nano-indenter compliant to ISO 14577 and ASTM E2546. Berkovich nano-indenter was used for characterisation. The loading rate of indenter (indenter velocity) affects contact hardness and Young's modulus of the materials [**24, 25**]. In this work, the loading rate of 1 μN/s was used. Multiple indentations were made in every specimen before arriving at the appropriate values as shown in **Table 2** and load-displacement (L-D) curves of all compositions are depicted in the **Fig. 5 (a) - (d)**. Mechanical properties of the specimens containing 0, 2.5, 5 and 10% WS_2 by weight in the low alloy steel are shown in **Table 2**. The shear bands which are occurring beneath the indenter tip provide information about dislocation source activation, shear instability initiation, defect nucleation and dynamics, mechanical instabilities or strain localization, and phase transformations. Continuous stiffness measurement technique based on nano-indentation was used satisfactorily for characterization of the materials [**26**]. The L-D curve was recorded as the indenter tip was pressed into the test material's surface. In L-D curves, not only the onward loading curve is important which is based on mathematical

properties of derivability and differentiability but also unloading curve to which main nano-mechanical and structural properties have been connected. Modeling on unloading curve using functional analysis of force, the concavity direction and the energetic properties of materials was reported [**27**]. On careful examination of L-D curves (**Fig. 5 (a) - (d)**), it was observed that the least displacement was found in PM-processed low alloy steel impregnated with 2.5 % WS_2 of all the specimens which shows higher amount of resistance due to bainitic phases in the microstructure between contact depth and contact stiffness values [**11**]. This could be due to possible phase transformation during nano-indentation [**28**]. From the results of nano-indentation, it was observed that low alloy steel impregnated with 2.5 % WS_2 was having highest hardness which could be attributed due to micro structural changes offering resistance.

From the microstructure, as we have seen, the phase transformations influence behavior of the diffusion bonded specimens [**29**]. From the results of

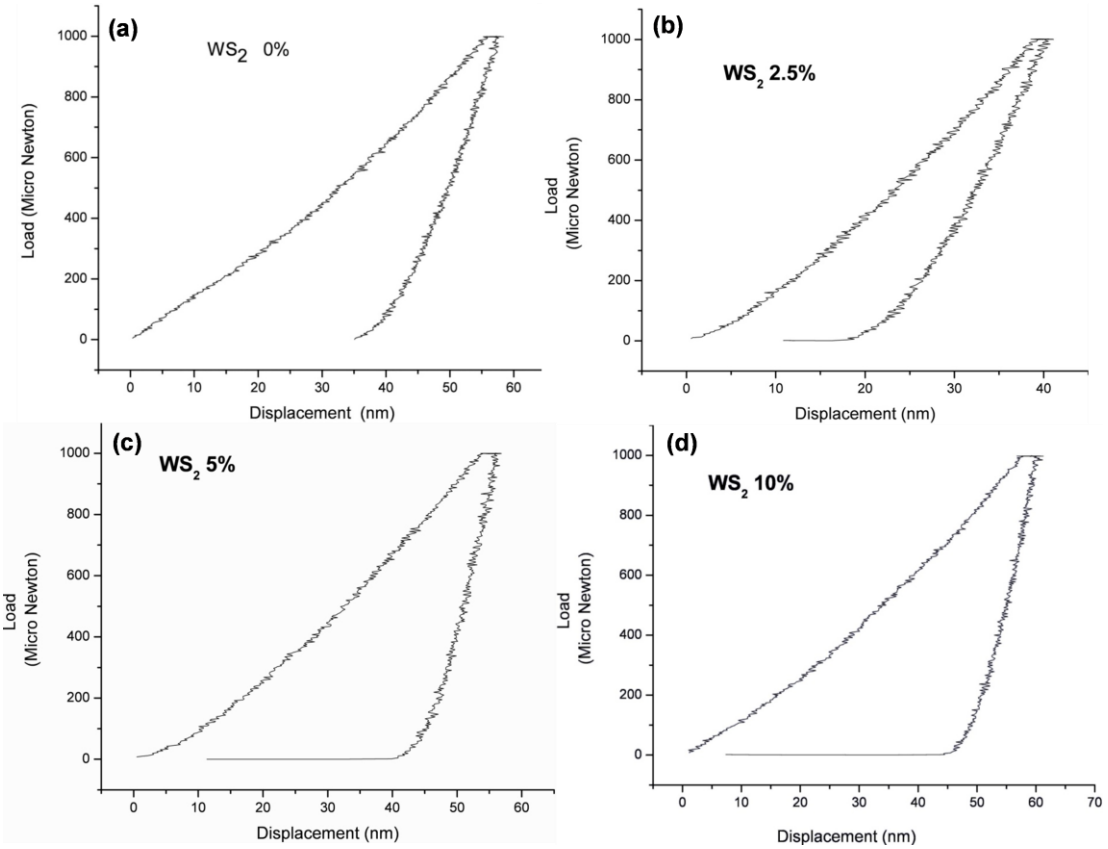

Fig. 5. L-D curve of low alloy steel: (a) without WS_2, (b) with 2.5% WS_2, (c) with 5% WS_2, and (d) with 10% WS_2.

(**Fig. 5(b)**). Similarly, much improved elastic behaviour of PM-processed low alloy steel impregnated with 2.5 % WS_2 (**Fig. 5(b)**) was observed from the unloading curves. The elastic modulus of the sintered specimen was found to be increasing with the increase in the content of the WS_2 in the composite at 2.5 % and then it was found to be decreasing with the further increase in WS_2. Similar trend was observed with hardness of the composites. The addition of the WS_2 was found to increase the ductility of the composites and resulted in increase in the contact depth of the indentation.

From the results, it was observed that contact stiffness was also increasing with the addition of WS_2 in the composite. The increase in the contact stiffness was more pronounced with 2.5 % WS_2. The contact depth and contact area were found to be the least with 2.5 % proportion of WS_2 in the composite. It was reported earlier that there was strong correlation nano-indentation shown in the **Table 2**, the highest amount of elastic modulus was observed in low alloy steel impregnated with 2.5 % WS_2 and this is attributed to bainitic phases with lesser porous microstructure, resulting in improved resistance for deformation. Even though martensitic phases were observed in the PM-processed low alloy steel with 5 and 10% WS_2, higher amount of porosity resulted in lesser resistance for deformation.

Table 2. Results of nano-indentation.

% WS_2 (by weight)	Elastic modulus (GPa)	Hardness (GPa)	Contact depth (nm)	Contact Stiffness (μN/nm)	Max. Force (μN)	Max. Depth (nm)	Contact Area (nm^2)
Zero	269.2	18.49	46.9	70.6	997.8	58.4	53971.7
2.5 %	433.6	16.90	49.1	118.8	997.0	56.4	58982.2
5 %	360.8	15.63	51.0	102.9	997.1	59.0	63802.4
10 %	333.2	11.59	59.2	110.2	995.1	66.8	85863.9

Conclusion

Nano-indentation technique was successfully used to characterize mechanical properties of WS_2-impregnated low alloy steel composites. There is close relationship among the indenter depth and the mechanical properties and micro structures of the specimens. The values of elastic moduli and contact stiffness were found to be higher in the PM-processed low alloy steel, impregnated with WS_2 compared to the specimen without WS_2. The rate of increase in the elastic moduli and contact stiffness was more pronounced initially i.e., with 2.5 % WS_2 when compared to further addition of WS_2. The specimen with 2.5 % WS_2 by weight has the highest hardness and the highest elastic modulus of all the proportions tested, which may be attributed to predominant bainitic structure in the low alloy steel specimen impregnated with 2.5 % WS_2. Contact depth of the indentation increases with the addition of the WS_2 above 2.5 % by weight due to increase in the porosity of the composites. Hence it is concluded to limit the addition of the WS_2 to 2.5 % by weight in the PM-processed low alloy steel for manufacturing sliding components.

Acknowledgements

The authors place on record their gratitude to Dr. R Subramanian, Professor, Department of Metallurgical Engineering, PSG College of Technology, Coimbatore, India for providing valuable suggestions for the article.

Author's contributions

Conceived the plan: Suresh R. Ambalam[1*], Rajendran I. Gounder[2]
Performed the experiments: Suresh R. Ambalam[1*]
Data analysis: Suresh R. Ambalam[1*], Rajendran I. Gounder[2]
Wrote the paper: Suresh R. Ambalam[1*]

Authors have no competing financial interests.

References

1. Koszela, W.; Pawlus, P.; Galda, L.; *Wear*, **2007**, *263*, 1585. **DOI:**10.1016/j.wear.2007.01.108
2. Ryk, G.; Etsion, I.; *Wear*, **2006,** *261*, 792. **DOI:**10.1016/j.wear.2006.01.031
3. Etsion, I.; Sher, E.; *Tribol. Int.*, **2009**, *42*, 542. **DOI:**10.1016/j.triboint.2008.02.015
4. Angelo, P. C.; Subramanian, R. (Eds.); Powder Metallurgy; PHI: India, **2009**. **ISBN-13**: 9788120332812
5. Fallahdoost, H.; Khorsand, H.; Eslami-Farsani, R.; Ganjeh, E.; *Mater. Des*., **2014**, *57*, 60. **DOI:**10.1016/j.matdes.2013.12.030
6. Salahinejad, E.; Amini, R.; Marasi, M.; Hadianfard, M. J.; *Mater. Des*., **2010**, *31*, 2259. **DOI:**10.1016/j.matdes.2009.10.008
7. Straffelini, G.; Benedetti, M.; Fontanari, V.; *Mater. Des*., **2014**, *61*, 101. **DOI:**10.1016/j.matdes.2014.04.027
8. Grimanelis, D.; Eyre, T. S.; *Wear*, **2007**, *262*, 93. **DOI:**10.1016/j.wear.2006.04.006
9. Shanmugasundaram, D.; Chandramouli, R.; *Mater. Des*., **2009**, *30*, 3444. **DOI:**10.1016/j.matdes.2009.03.020
10. Fischer-Cripps, A. C.; *Surf. Coat. Technol.*, **2006**, *200*, 4153. **DOI:**10.1016/j.surfcoat.2005.03.018
11. Taylor, M. D.; Choi, K. S.; Sun, X.; Matlock, D. K.; Packard, C. E.; Xu, L.; Barlat, F.; *Mater. Sci. Eng., A*, **2014**, *597*, 431. **DOI:**10.1016/j.msea.2013.12.084
12. Oliver, W. C.; Pharr, G. M.; *J. Mater. Res*., **2004**, *19*, 3. **DOI:**10.1557/jmr.2004.19.1.3
13. Baltazar Hernandez, V. H.; Panda, S. K.; Kuntz, M. L.; Zhou, Y.; *Mater. Lett.*, **2010**, *64*, 207. **DOI:**10.1016/j.matlet.2009.10.040
14. Dey, A.; Mukhopadhyay, A. K. (Eds.); Nano Indentation of Brittle Solids; CRC Press: USA, **2014**. **ISBN-13**: 9781466596900
15. Liu, M.; Lu, C.; Tieu, K.; Yu, H.; *Mater. Sci. Eng. A*, **2014**, *619*, 57. **DOI:**10.1016/j.msea.2014.09.034
16. Gong, J.; Miao, H.; Peng, Z.; *Mater. Lett.*, **2004**, *58*, 1349. **DOI:**10.1016/j.matlet.2003.09.026
17. Lashgari, H. R.; Chen, Z.; Liao, X. Z.; Chu, D.; Ferry, M.; Li, S.; *Mater. Sci. Eng., A*, **2015**, *626*, 480. **DOI:**10.1016/j.msea.2014.12.097
18. Tiwari, A. (Eds.); Applied Nano indentation in Advanced Materials; Wiley-Blackwell: UK, **2016**. **ISBN-13:** 9781119084495
19. Roa, J. J.; Jiménez-Piqué, E.; Tarragó, J. M.; Zivcec, M.; Broeckmann, C.; Llanes, L.; *Mater. Sci. Eng., A*, **2015**, *621*, 128. **DOI:**10.1016/j.msea.2014.10.064
20. Králík, V.; Němeček, J.; *Mater. Sci. Eng., A*, **2014**, *618*, 118. **DOI:**10.1016/j.msea.2014.08.036
21. Shaham, D.; Rawers, J.; Zolotoyabko, E; *Mater. Lett*., **1996**, *27*, 41. **DOI:**10.1016/0167-577x(95)00274-x
22. Han, F.; Tang, B.; Kou, H.; Li, J.; Feng, Y.; *Mater. Sci. Eng., A*, **2015**, *625*, 28. **DOI:**10.1016/j.msea.2014.11.090
23. Voyiadjis, G. Z.; Zhang, C.; *Mater. Sci. Eng., A*, **2015**, *62*, 139. **DOI:**10.1016/j.msea.2014.10.070
24. Alao, A. -R.; Yin, L.; *Mater. Sci. Eng., A*, **2015**, *628*, 181. **DOI:**10.1016/j.msea.2015.01.051
25. Alao, A. -R.; Yin, L.; *Mater. Sci. Eng., A*, **2014**, *619*, 247. **DOI:**10.1016/j.msea.2014.09.101
26. Li, X.; Bhushan, B.; *Mater. Charact*., **2002**, *48*, 11. **DOI:**10.1016/s1044-5803(02)00192-4
27. Attaf, M. T.; *Mater. Lett.*, **2004**, *58*, 507. **DOI:**10.1016/s0167-577x(03)00535-4
28. Sadeghpour, S.; Kermanpur, A.; Najafizadeh, A.; *Mater. Sci. Eng., A*, **2014**, 612, 214. **DOI:**10.1016/j.msea.2014.06.055
29. Abdoos, H.; Khorsand, H.; Shahani, A. R.; *Mater. Des*., **2009**, *30*, 1026. **DOI:**10.1016/j.matdes.2008.06.050.

